Two-Dimensional Electrolyte Nature of Exfoliated Montmorillonite Nanoplatelets Fabricated by Soap-Free Emulsion Polymerization and Their Affinity for Cations

Chia-Hsin Lee,[1] Ting Hsiang Weng,[1] Ken Yen Liu,[1] Keng Jen Lin,[2] King-Fu Lin[1,2]

[1]*Department of Materials Science and Engineering, National Taiwan University, Taipei, Taiwan, Republic of China*
[2]*Institute of Polymer Science and Engineering, National Taiwan University, Taipei Taiwan, Republic of China*

Received 29 October 2009; accepted 6 March 2010
DOI 10.1002/app.32390
Published online 24 May 2010 in Wiley InterScience (www.interscience.wiley.com).

ABSTRACT: Montmorillonite (MMT) nanoplatelets, fabricated by the exfoliation of MMT during participating in the soap-free emulsion polymerization of methyl methacrylate, were well-dispersed in water and performed like a two-dimensional electrolyte. Their ionic conductivity roughly follows the Manning's limiting law for the conduction of a polyelectrolyte. The dissociated MMT nanoplatelets that carry negative charges in water were able to rapidly adsorb cations, such as tris(2,2′-bipyridyl)ruthenium(II) ($Ru(bpy)_3^{2+}$) and methylene blue (MB^+), and recover into a smectic configuration floating as a separating phase. By using the Langmuir equation, we were able to estimate the occupied surface areas of MMT nanoplatelets by each $Ru(bpy)_3^{2+}$ and MB^+ cations as 4.708 and 1.806 nm^2/ion, respectively. © 2010 Wiley Periodicals, Inc. J Appl Polym Sci 118: 652–658, 2010

Key words: montmorillonite; clay; electrolytes; cations; encapsulation

INTRODUCTION

Montmorillonite (MMT) is a mica-type smectic clay of stacking several nanoplatelets, each of which consists of two tetrahedral silica layers fusing into an edge-shared octahedral layer of alumina.[1,2] Recently, we have discovered a novel method to exfoliate MMT during soap-free emulsion polymerization in the presence of MMT to fabricate the nanocomposite latices.[3–10] It has been verified that the polymerizing chains diffused into the interlayer region of MMT and formed a disk-like micelle that triggered the exfoliation.[3,4]

In this study, by removal of the poly(methylmethacrylate) (PMMA) matrix from the exfoliated MMT/PMMA nanocomposite latex particles with toluene, we were able to collect the MMT nanoplatelets. The exfoliated MMT nanoplatelets act like a two-dimensional electrolyte in water carrying negative charges. Its ionic conductivity in aqueous solution roughly follows the Manning's limiting law[11] for the conduction of a polyelectrolyte. As it was mixed with organic cations such as tris(2,2′-bipyridyl)ruthenium(II) ($Ru(bpy)_3^{2+}$) and methylene blue (MB^+) in water, they rapidly organized into a smectic configuration. Notably, by using the Langmuir equation, we were able to estimate the occupied surface areas of MMT nanoplatelets by those cations.

EXPERIMENTAL

Materials

Montmorillonite (MMT, PK-802) with cationic exchange capacitiy (CEC) = 114 meq/100 g was purchased from PAI KONG Nanotechnology in Taiwan. Methyl methacrylate (MMA, Acros) was distilled under vacuum and only intermediate distillate was used. Tris(2,2′-bipyridyl)dichlororuthenium(II) hexahydrate ($Ru(bpy)_3Cl_26H_2O$, Aldrich, Milwaukee, WI) and MB (Acros, Geel, Belgium) were used without further treatment. The water used for entire study was purified to 18.3 MΩ by a Barnstead Easypure RF system.

Sample preparation

The preparation method of exfoliated MMT/PMMA nanocomposite latex has been described elsewhere.[3] In general, to a three-neck flask that has been loaded with 125 mL water was added 0.3852 g potassium persulfate (KPS, Acros) initiator and 0.5 g MMT. After stirring at room temperature overnight, 9.5 g MMA monomer was added. The solution was then heated to 70°C for ~ 3 h until no further

Correspondence to: K.-F. Lin (kflin@ntu.edu.tw).
Contract grant sponsor: The National Science Council in Taiwan, Republic of China; contract grant number: NSC96-2221-E-002-144-MY3.

© 2010 Wiley Periodicals, Inc.

polymerization was detected. Exfoliated MMT/PMMA nanocomposite latex particles were obtained by centrifuging the solution to remove water.

To prepare the exfoliated MMT nanoplatelets, ~ 10 g of latex particles were added to 200 mL of toluene, which was then heated to 120°C with stirring in an autoclave and maintained at ~ 200 psi for 6 h. After cooling, ~ 500 mL of water was added to extract the exfoliated MMT nanoplatelets from the toluene solution. The solution was stirred for 2 h and then left undisturbed until it gets separated into two phases. The aqueous phase in the lower part was collected and then concentrated to ~ 1 wt % MMT nanoplatelets by evaporation. To prepare the sample for thermal gravimatric analysis (TGA), ~ 5 mL of the solution was taken and dried to a constant weight. To prepare the sample for TEM investigation, several drops of the solution was taken and diluted 10 folds with water. A carbon film-coated copper grid was dipped into the solution, withdrawn immediately, and dried in a desiccator. To prepare the sample for conductivity measurements, the aqueous solution was subjected to dialysis in a Spectra/Pro regenerated cellulose membrane tube against water to remove the small salts.[12] The cutoff molecular weight was 3,500. The solution was dialyzed until the conductivity of the repeatedly refreshed water surrounding the dialysis tube close to 1 μs/cm. The concentration of MMT nanoplatelets in aqueous solution after dialysis was 8.83×10^{-2} wt %, measured by weight change after drying to a constant weight at ~ 150°C. It was then gradually diluted to several desired concentrations with water.

Methods

TGA was carried out in a TA Instruments model SDT Q600 thermal gravimetric analyzer at a heating rate of 10°C/min under nitrogen. The conductivity measurement of the exfoliated MMT aqueous solutions, which were thermostated at 30°C with a deviation of 0.01°C, was performed with a Radiometer Copenhagen CDC-230 conductivity meter. The adsorptions of MMT nanoplatelets in aqueous solutions by $Ru(bpy)_3^{2+}$ and MB^+, respectively were carried out by the following method. First, 1.5 mL of 0.36 wt % exfoliated MMT aqueous solution was added to 1.5 mL aqueous solutions of $Ru(bpy)_3Cl_2$ and MB, respectively with various concentrations. Both solutions were immediately separated into two phases. To allow the adsorption more completely, the solutions were stirred for 1 day and then filtered through a 0.2 μm filter. The filtrate was collected and subjected to the measurement of UV/vis spectroscopy with a JASCO-555 UV/vis spectrophotometer. The intensities of absorption peaks at 455 and 664 nm wavelengths were chosen to estimate the concentration of the remaining unadsorbed $Ru(bpy)_3^{+2}$ and MB^+, respectively. The linear plots of peak intensities versus the known concentrations of respective $Ru(bpy)_3^{2+}$ and MB^+ were established for calibration. The remaining larger particles that could not pass through the filter were dried at 80°C and subjected to the X-ray diffraction and TEM investigations. The samples for TEM were dispersed in water and a carbon film-coated copper grid was dipped into the solution, withdrawn immediately, and dried in a desiccator. TEM images were investigated with a JEOL JSM-1230 transmission electron microscope. X-ray diffraction patterns (XRD) were recorded on a PANalytical X'Pert Pro X-ray diffraction analyzer with nickel-filtered Cu Kα radiation at 45 kV and 40 mA.

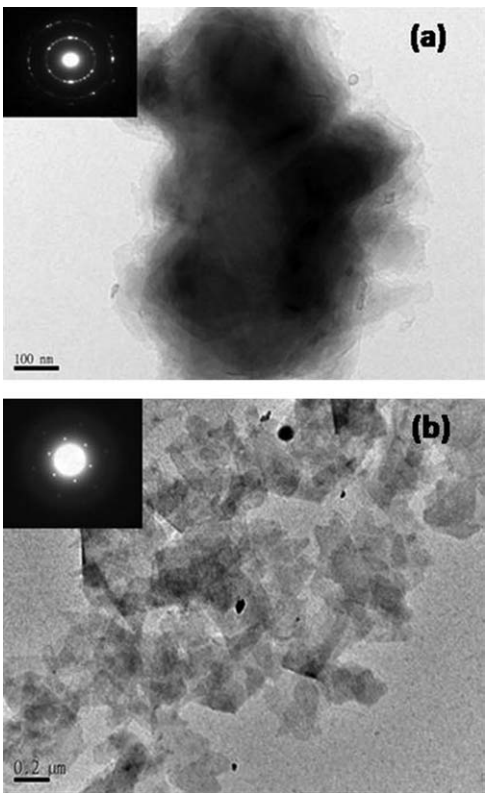

Figure 1 TEM images and electron diffraction patterns of (a) pristine MMT and (b) exfoliated MMT nanoplatelets.

RESULTS AND DISCUSSION

Exfoliated MMT nanoplatelets

As the exfoliated MMT nanoplatelets were extracted from the MMT/PMMA nanocomposite latex, they dispersed homogeneously in water. Figure 1 shows the TEM images of pristine MMT and its exfoliated nanoplatelets along with their respective electronic diffraction patterns. Pristine MMT is a mica-like smectic clay and its electron diffraction is basically a ring pattern as shown in Figure 1(a). As MMT was

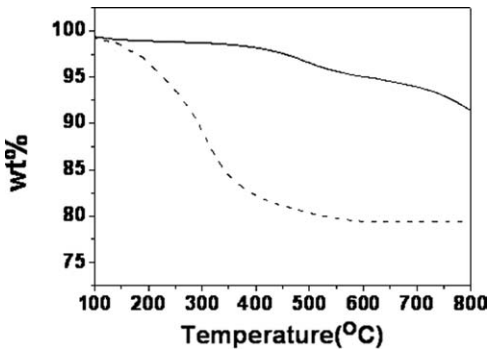

Figure 2 TGA plots of (—) pristine MMT and (---)exfoliated MMT nanoplatelets after removal of PMMA matrix with toluene.

exfoliated into nanoplatelets, the electron diffraction altered into a six-fold symmetric spot pattern [see Fig. 1(b)], indicating that they are a hexagonal single-crystal. Similar electron diffraction pattern from a MMT nanoplatelet was also reported by Vaia and coworkers.[13] Obviously, the original ring pattern of MMT was mainly resulted from the packing of nanoplatelets.

Figure 2 shows the TGA plots of the exfoliated MMT nanoplatelets along with the pristine MMT for comparison. The remaining PMMA matrix on the exfoliated MMT nanoplatelets, which was not dissolvable in toluene but decomposed after heating to 500°C, was estimated to be about 17 wt %.

It has been verified for the exfoliated MMT/poly(methylacrylate-co-methylmethacrylate) nanocomposite latex prepared by the similar method that the polymer chains have been grafted onto the exfoliated MMT nanoplateltes so that they cannot be removed by toluene.[14] MMT used for this study has a CEC value of 114 meq/100 g, by that each exfoliated MMT nanoplatelet was estimated to carry 1.78 monovalent groups per nanometer square under an assumption that each nanoplatelet has a thickness of 1 nm with a density of 2.6 g/cm^3.[15] As they disperse in water, they carry negative charges with dissociated cations as a counterion. Because MMT has been mixed with five CEC of KPS initiator to prepare the exfoliated MMT/PMMA nanocomposite latex, the majority of counterions would be potassium ions. Before the aqueous solutions of exfoliated MMT nanoplatelets were subjected to measure the ionic conductivity, they were dialyzed against water to remove the excess small salts for purification.

Figure 3 shows the double-logarithmic plot of equivalent ionic conductivity of MMT nanoplatelets versus concentration in aqueous solution at 30°C. The equivalent ionic conductivity was increased by decreasing the concentration, similar to the behavior of polyelectrolyte in aqueous solution.[16–18] Manning has derived a limiting law to predict the ionic conduction of a polyelectrolyte by assuming that the hydrodynamic interactions between segments of the chain distant along the contour are absent.[11] To simplify the theoretical argument for our system, the MMT nanoplatelets were hypothetically considered as a two-dimensional square lattice and that the ions are arrayed similar to the paralleled polyions with a distance equal to the average charge spacing b = 0.75 nm, estimated from the number of monovalent groups per nanometer square in average, which is $(1/1.78)^{1/2} = 0.75$.

The line charge density ξ of polyions with monovalent groups has been defined by $\xi = l_B/b$, where l_B is the Bjerrum length, given by[19]

$$l_B = \frac{e^2}{4\pi\varepsilon_0\varepsilon KT} \tag{1}$$

in which e is the electronic charge, ε is the dielectric constant of solvent (water in our case), $4\pi\varepsilon_0$ is the permeability of the vacuum, K is the Bolzmann constant, and T is the temperature. For water at 30°C (ε = 76.75), l_B = 7.173 Å. According to the Manning's limiting law,[20] if $\xi > 1$, the counter ions will condense until $\xi = 1$. If $\xi < 1$, the counter ions will be fully dissociate. In our case, ξ = 0.956. The potassium counterions of exfoliated MMT nanoplatelets should be fully dissociated.

Assuming that the interactions between MMT nanoplatelets and dissociated potassium ions are only Debye-Hückel interactions, the molar ionic conductivity Λ_m of the MMT nanoplatelets in aqueous solution can be estimated by,[11]

$$\Lambda_m = f(\Lambda_{K^+} + \Lambda_{MMT^-}) \tag{2}$$

where f is the average self-diffusion coefficient of the counterions divided by that in the MMT-free solution, which has been derived for $\xi < 1$ in the polyelectrolyte system as[20]

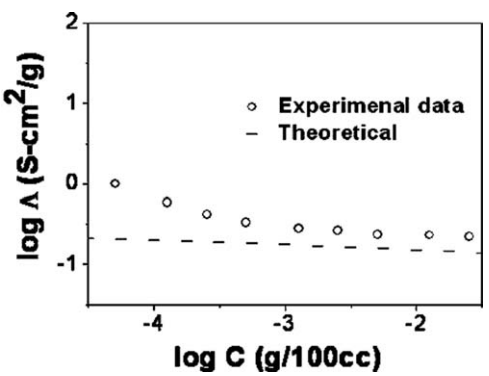

Figure 3 Double-logarithmic plots of equivalent conductivity of MMT nanoplatelets versus concentration.

Figure 4 Photographs of (1) 0.36 wt % exfoliated MMT in water, (2) 1×10^{-4} M $Ru(bpy)_3Cl_2$ in water, (3) immediately mixed soluiton of (1) and (2), and (4) the filtrate of solution (3) after passing through a 0.2 μm filter. [Color figure can be viewed in the online issue, which is available at www.interscience.wiley.com.]

$$f = 1 - \frac{0.55\xi^2}{\pi + \xi} \tag{3}$$

Λ_{K^+} is the molar ionic conductivity of K^+ ions equal to 73.5 ($S \cdot cm^2/mol$),[21] and Λ_{MMT^-} is the molar ionic conductivity of MMT^- ions. From eq. (3), $f = 0.882$ was obtained. Besides, Λ_{MMT^-} can be theoretically estimated by

$$\Lambda_{MMT^-} = FU \tag{4}$$

where F is the Faraday constant and U is the electrophoretic mobility of MMT nanoplatelet ions. In the salt-free MMT nanoplatelet aqueous solution case, the average charge spacing b is much smaller than Debye screening length κ^{-1} given by

$$\kappa^{-1} = (\varepsilon_o \varepsilon KT/2000 N_A c e^2)^{1/2} \tag{5}$$

in which c is the molar concentration of MMT nanoplatelet ions and N_A is Avogadro number. It indicates that the hydrodynamic interactions between charges are unscreened within the characteristic length κ^{-1}. According to the Manning's limiting law for the electrophoretic mobility of polyions,[11] as $\kappa b \ll 1$, the electrophoretic mobility U of MMT can be estimated by

$$300U = (4\varepsilon_o \varepsilon KT/3\eta e)|\ln(\kappa b)| \tag{6}$$

where η is the viscosity of water. From eqs. (2) and (4–6), the theoretical prediction value for Λ_m as a function of c can be calculated. Finally, based on the CEC value of MMT, we could convert Λ_m to Λ, which was included in Figure 3 for comparison. Although the prediction values are slightly lower than the experimental data, they are roughly parallel with each other, implying that our previous two-dimensional square lattice assumption for the ions in the MMT nanoplatelets is basically feasible.

Adsorption isotherm of MMT nanoplatelets

Adsorption isotherm of cations onto MMT has been studied for more than two decades.[22–24] However, it has a limitation for practical use, because diffusion of the cations into the interlayer regions of MMT for cationic exchange is time consuming.[22] In this study, we used the exfoliated MMT nanoplatelets to adsorb $Ru(bpy)_3^{2+}$ and MB^+, respectively in water. They formed a complex, floating as a separate phase almost immediately. Figure 4 shows the photographs of exfoliated MMT aqueous solution, $Ru(bpy)_3Cl_2$ aqueous solution, and their immediately mixed

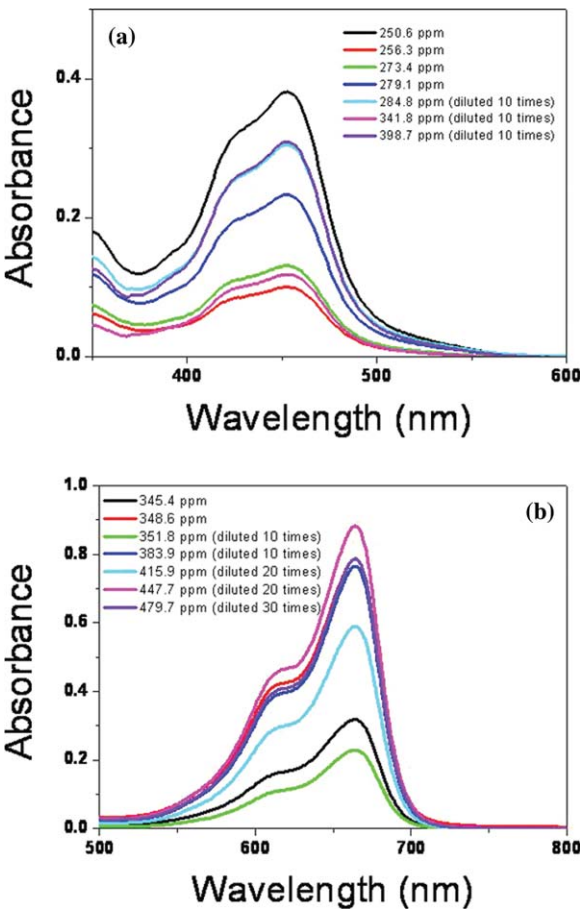

Figure 5 UV/vis spectra of (a) $Ru(bpy)_3Cl_2$ and (b) MB aqueous solutions (with the indicated initial concentrations C_o) after mixing with the exfoliated MMT in water and passing through a 0.2 μm filter. Note: Some of the data have been diluted as indicated in the figures to better fit the calibration curve. [Color figure can be viewed in the online issue, which is available at www.interscience.wiley.com.]

TABLE I
Adsorption Data of $Ru(bpy)_3^{2+}$ Onto the Exfoliated MMT Nanoplatelets

C_0 (ppm)	C_e (ppm)	q_e (mg/g)	Ce/q_e (g/L)
256.3	3.9	140.2	0.028
273.4	5.2	149	0.035
279.1	9.3	149.9	0.062
284.8	12.2	151.4	0.080
250.6	15.2	130.8	0.116
341.8	47.2	163.7	0.288
398.7	123.5	152.9	0.808

solution. To allow the adsorption to reach equilibrium, the mixed solutions have been stirred overnight and then filtered through a 0.2 μm filter. The filtrates were collected and subjected to measure the remaining concentrations of unadsorbed $Ru(bpy)_3^{2+}$ and MB^+, respectively by UV/vis spectroscopy as shown in Figure 5. The intensities of absorption peaks at 455 and 664 nm wavelengths were chosen to estimate the concentration C_e of the remaining unadsorbed $Ru(bpy)_3{}^{+2}$ and MB^+, respectively, the results of which are listed in Tables I and II. To realize if the adsorptions of respective $Ru(bpy)_3^{2+}$ and MB^+ onto the MMT nanoplatelets follow the Langmuir isotherms, we plotted C_e/q_e vs. C_e, where q_e is the weight of adsorbed cations divided by the weight of exfoliated MMT. Good linear plots (R^2 = 0.99) of the data points were obtained (see Fig. 6), which can be fit perfectly by the Langmuir equation,[25]

$$\frac{C_e}{q_e} = mC_e + b \tag{7}$$

where m and b are constants. The m and b data for the adsorptions of respective $Ru(bpy)_3^{2+}$ and MB^+ on the MMT nanoplatelets in Figure 6 fitted by eq. (7) are listed in Table III. By changing the unit of C_e to molarity and that of q_e to mole/g in eq. (7), the values of m can be assigned a physical significance by[25]

$$m = \frac{N_A \sigma^0}{A_{sp}} \tag{8}$$

TABLE II
Adsorption Data of MB^+ Onto the Exfoliated MMT Nanoplatelets

C_0 (ppm)	C_e (ppm)	q_e (mg/g)	C_e/q_e
345.4	1.58	191	0.008
348.6	3.9	191.5	0.020
351.8	11.39	189.1	0.060
383.9	37.9	192.2	0.197
415.8	58.53	198.5	0.294
447.7	87.54	200.1	0.437
479.7	117.03	201.5	0.581

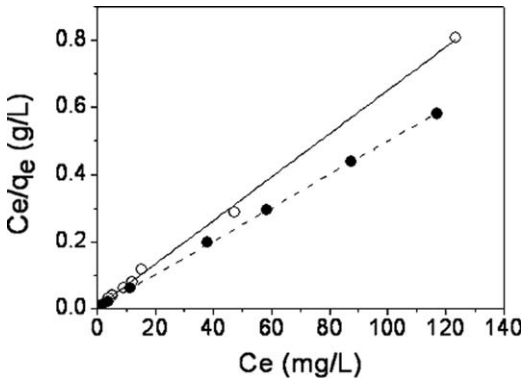

Figure 6 C_e/q_e of (○) $Ru(bpy)_3^{2+}$ and (●) MB^+ vs. concentrations. The lines were obtained by fitting the data with the first least-squares method (R^2 = 0.99).

where σ^o is the area occupied per ion and A_{sp} is the specific area of the adsorbent, that is, the exfoliated MMT nanoplatelets in our case. Based on our previous assumption that each nanoplatelet has a thickness of 1 nm with a density of 2.6 g/cm^3,[15] A_{sp} is equal to 769.2 m^2/g. Thus, σ^o can be calculated by eq. (8) as 4.708 and 1.806 nm^2/ion for $Ru(bpy)_3^{2+}$ and MB^+, respectively. The σ^o of $Ru(bpy)_3^{2+}$ adsorbed on exfoliated MMT nanoplatelets in our experiment is slightly larger than that reported by Villemure,[26] who mixed $Ru(bpy)_3Cl_2$ with pristine MMT (A_{sp} = 750 m^2/g) for 48 h and obtained σ^o = 3.5 nm^2. The σ^o of MB^+ adsorbed on exfoliated MMT nanoplatelets in our experiment is also larger than that reported by Suter and coworkers[27] who mixed MB with Mica (A_{sp} = 107 m^2/g) and obtained σ^o = 0.66 nm^2. However, the authors claimed that MB^+ to adsorb onto the mica was through the edge-on intercalation, because the flat surface area of MB^+ is 1.338 nm^2. This edge-on intercalation to mica has also been supported by other researchers.[28]

The MMT/$Ru(bpy)_3{}^{+2}$ and MMT/MB^+ complexes that could not pass through the filter after drying were then subjected to the wide-angle X-ray diffraction and TEM investigations. Figure 7 shows their XRD patterns along with those of pristine MMT and exfoliated MMT nanoplatelets for comparison. The characteristic diffraction peak at $2\theta = 7.2^o$ for pristine MMT corresponding to the d_{001}-spacing of 12.3 Å was completely vanished as it was exfoliated to MMT nanoplatelets. However, the MMT/$Ru(bpy)_3{}^{+2}$ and MMT/MB^+ complexes have the characteristic peak reappeared at $2\theta = 5.41^o$ and 3.90^o,

TABLE III
Langmuir Equation Data for $Ru(bpy)_3^{2+}$ and MB^+, Respectively, Adsorbing Onto the MMT Nanoplatelets

	m (g/mg)	b (g/L)	σ° (nm)^2
$Ru(bpy)_3^{2+}$	0.00647	0.00371	4.708
Methylene blue	0.00497	0.00188	1.806

corresponding to the d_{001}-spacings of 16.3 and 22.6 Å respectively. Notably, the pristine MMTs adsorbing $Ru(bpy)_3^{+2}$ and MB^+ through intercalation were reported to have the d_{001}-spacings of 17.9 and 22 Å,[24,29] respectively similar to our results. This phenomenon suggested that the exfoliated MMT nanoplateles could restack with each other in the presence of cations by Columbus attractive force. Notably, because diffusion of the cations into the interlayer regions of pristine MMT for cationic exchange is time consuming, it has a limitation for practical use.[22] In this study, we used the exfoliated MMT nanoplatelets to adsorb $Ru(bpy)_3^{2+}$ and MB^+, respectively in water. They formed a complex floating as a separate phase almost immediately.

Figure 8 shows the TEM image of MMT/$Ru(bpy)_3^{2+}$ complex with its electron diffraction pattern. Although the MMT nanoplatelets have restacked into a smetic configuration, the electron diffraction pattern did not show a complete ring pattern, indicating that the MMT nanoplatelets of MMT/$Ru(bpy)_3^{2+}$ complex are not so well-packed as the pristine MMT. The Moiré fringe pattern appeared in the higher magnified image [see Fig. 8(b)], which has not been found for the pristine MMT also reveals its misaligned stacking of single crystalline MMT nanoplatelets. Similar TEM image was also found for the MMT/MB^+ complex.

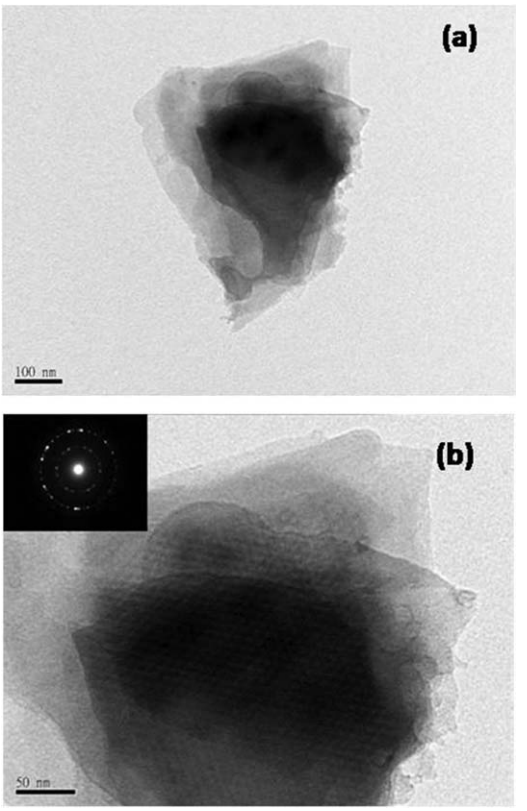

Figure 8 TEM images of MMT/$Ru(bpy)_3^{2+}$ complex; (a) low-magnification and (b) high-magnification with diffraction pattern.

CONCLUSIONS

The exfoliated MMT nanoplatelets not only act as a two-dimensional electrolyte but also perform like a scavenger for the cations in aqueous solution. Their ionic conductivity in aqueous solution roughly follows the Manning's limiting law for the conduction of a polyelectrolyte. As the MMT nanoplatelets were mixed with $Ru(bpy)_3^{2+}$ and MB^+, respectively in water, they formed an intercalated smectic complex floating as a separate phase almost immediately. By using the Langmuir equation, we were able to estimate the occupied surface areas of MMT nanoplatelets by each $Ru(bpy)_3^{2+}$ and MB^+ cations as 4.708 and 1.806 nm^2/ion, respectively.

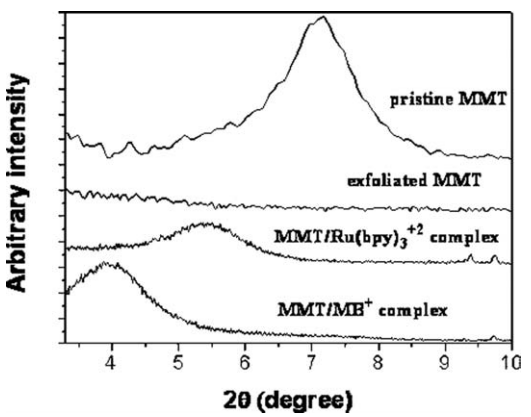

Figure 7 XRD Patterns of pristine MMT, exfoliated MMT, and MMT/$Ru(bpy)_3^{2+}$ and MMT/MB^+ complexes.

References

1. Chen, C.; Curliss, D. Nanotechnology 2003, 14, 643.
2. Ray, S. S.; Okamoto, M. Prog Polym Sci 2003, 28, 1539.
3. Lin, K. F.; Lin, S. C.; Chien, A. T.; Hsieh, C. C.; Yen, M. H.; Lee, C. H.; Lin, C. S.; Chiu, W. Y.; Lee, Y. H. J Polym Sci Part A: Polym Chem 2006, 44, 5572.
4. Lin, K. J.; Dai, C. A.; Lin, K. F. J Polym Sci Part A: Polym Chem 2009, 47, 459.
5. Chien, A. T.; Lin, K. F. J Polym Sci Part A: Polym Chem 2007, 45, 5583.
6. Chien, A. T.; Lee, Y. H.; Lin, K. F. J Appl Polym Sci 2007, 106, 355.
7. Lin, K. F.; Hsu, C. Y.; Huang, T. S.; Chiu, W. Y.; Lee, Y. H.; Young, T. H. J Appl Polym Sci 2005, 98, 2042.
8. Lee, Y. H.; Chien, A. T.; Yen, M. H.; Lin, K. F. J Polym Res 2008, 15, 31.
9. Yen, M. H.; Lin, K. F. J Polym Sci Part B: Polym Phys 2009, 47, 524.
10. Lin, K. J.; Lee, C. H.; Lin, K. F. J Polym Sci Part B: Polym Phys, to appear.
11. Manning, G. S. J Phys Chem 1981, 85, 1506.
12. Lin, K. F.; Yang, S. N.; Cheng, H. L.; Cheng, Y. H. Macromolecules 1999, 32, 4602.
13. Drummy, L. F.; Koerner, H.; Farmer, K.; Tan, A.; Farmer, B. L.; Vaia, R. A. J Phys Chem B 2005, 109, 17868.

14. Lin, K. J.; Weng, T. H.; Lee, C. H.; Lin, K. F. J Polym Sci Part A: Polym Chem 2009, 47, 5891.
15. Tu, C. W.; Liu, K. Y.; Chien, A. T.; Yen, M. H.; Weng, T. H.; Ho, K. C.; Lin, K. F. J Polym Sci Part A: Polym Chem 2008, 46, 47.
16. Cheng, H. L.; Lin, K. F. Langmuir 2002, 18, 7287.
17. Cheng, H. L.; Lin, K. F. Macromolecules 2003, 36, 6949.
18. Lin, K. F.; Cheng, H. L.; Cheng, Y. H. Polymer 2004, 45, 2387.
19. Manning, G. S. J Chem Phys 1969, 51, 924.
20. Manning, G. S. J Chem Phys 1969, 51, 934.
21. Atkins, P. W. Physical Chemistry, 5th ed.; Oxford University Press: Oxford, 1994.
22. Jaynes, W. F.; Bigham, J. M. Clays Clay Miner 1986, 38, 93.
23. Narkiewicz-Michalek, J. Langmuir 1992, 8, 7.
24. Kaneko, Y.; Iyia, N.; Bujdák, J.; Sasai, R.; Fujita, T. J Mater Res 2003, 18, 2639.
25. Hiemenz, P. C. Principle of Colloid and Surface Chemistry, 2nd ed.; Marcel Dekker: New York, 1986.
26. Villemure, G. Clays Clay Miner 1990, 38, 622.
27. Shelden, R. A.; Caseri, W. R.; Suter, U. W. J Colloid Interface Sci 1993, 157, 318.
28. Hähner, G.; Marti, A.; Spencer, N. D. J Chem Phys 1996, 104, 7749.
29. Villemure, G. Clays Clay Miner 1991, 39, 580.